NANOSCALE CHARACTERIZATION OF BONE TISSUE UNDER A PRECISE DISPLACEMENT CONTROL USING ATOMIC FORCE MICROSCOPY

Undergraduate Honors Thesis

Presented in Partial Fulfillment of the Requirements for

Graduation with Distinction in the

Department of Mechanical Engineering at

The Ohio State University

Zhi Zhang

May 2017

Advisor: Hanna Cho, Ph.D.

Abstract

The bone is an indispensable structure in the skeletal system of the human body that provides a mechanical function to bear various loadings. In a healthy person or animal, bone remodels its composition and arrangement of the constituent materials to adapt to changing functional demands continuously throughout life [1]. However, the mechanism of how the force input to the bone is transduced to be involved in the physiological bone buildup process has not been clearly understood. In order to uncover the mechanism, this project aims to investigate the changes in the morphology and properties of bone in response to an external loading stimuli using Atomic Force Microscopy (AFM). To achieve this goal, a precise displacement control is integrated into an existing AFM setup. A piezoelectric motor with a nanometer-scale resolution provides a precise control of force and displacement while the force load data is acquired by an axial tension load cell integrated in the stage. The successful integration of the force and displacement control into AFM enables to image the bone sample with the nanometer-scale resolution when a precisely controlled force is applied to the bone sample. The nanoscale morphology change of a human mandible bone sample is characterized while the strain of the sample valued between 0 and 0.001.

Acknowledgements

First and foremost, I would like to thank my advisor, Dr. Hanna Cho from bottom of my heart. She has always been willing to discuss the project, brainstorm ideas, and provide guidance and support.

I would like to thank Jinha for giving me suggestions and discussing the stage design with me. I really appreciate his explanations and bi-weekly meetings.

I would like to thank Sajith for his generous help and patience during the process of scanning bone samples.

I would like to thank Aaron Orsborn in the Scott Lab student machine shop for teaching me how to use the machines in the shop and providing support when needed.

I would like to thank Kevin Wolf and Chad Bivens in the Scott Lab machine shop. They provided countless tips and advice on the construction of my design.

Table of Contents

Abstract 2
Acknowledgements 3
Table of Contents 5
Table of Figures 6
Chapter 1: Introduction 7
1.1 Background 7
1.2 Bone Mineralization 9
1.3 Hypothesis 10
1.4 Objectives 11
1.5 Description of Atomic Force Microscopy (AFM) 12
Chapter 2: Design and Fabrication of Stage 14
2.1 Constrains 14
2.3.1 Conceptual design 15
2.3.2: 3-D Model 16
2.3.3: manufacturing and assembling 17
2.4 Control program 18
2.4.2 The user interface of the program 19
Chapter 3: Introduction of equipment 20
3.1 Atomic Force Microscopy (AFM) 20
3.2 Actuator 20
3.3 Linear Translation Stage and controller 21
Chapter 4: Characterization 22
4.1 Test the stage by probing toothpick sticks 22
4.2 Bone sample 24
4.2.1 Raw bone sample 25
4.2.2 Bone sample polished 27
Chapter 5: Summary 30
Chapter 6: Future Work 31
6.1 Improvement of the stage 31
6.2 Characterization and analysis of bone 32
Bibliography 33
Appendix 34

Table of Figures

Figure 1: The hierarchical structure of bone [1] 7
Figure 2: The comparison of normal bone and osteoporosis bone [3] 8
Figure 3: Wolff's Law [4] 9
Figure 4: Diagram of bone mineralization profile of new bone formation [5] 10
Figure 5: The general schematic of piezoelectric effect under force 11
Figure 6: The schematic of Atomic Force Microscope 13
Figure 7: AFM images of the surface of a mouse femur 13
Figure 10: The image of limitation height of AFM head 16
Figure 11: The isometric view of assembled stage in SOILDWORKS 17
Figure 12: The side view of assembly 17
Figure 13: The connected stage system 18
Figure 15: The user's interface of the program 19
Figure 16: The resolution of actuator corresponding to different load [7] 20
Figure 17: The experimental setup 22
Figure 18: The camera view from AFM 23
Figure 20: The dimension of mouse femur 25
Figure 21: the morphology of mouse femur without 1 μm input 25
Figure 22: The morphology of mouse femur without 1 μm input (detail) 26
Figure 23: The morphology of mouse femur with 1 μm input 26
Figure 24: The morphology of mouse femur with 1 μm input (detail) 27
Figure 26: The setup of stage with mouse femur 27
Figure 27: The morphology of mouse femur without strain input 28
Figure 28: The comparison of morphology of mouse femur 28
Figure 29: The front view of the stage 31
Figure 30: The comparison of designs 32
Figure 31: The drawing fixed support 34
Figure 32: The drawing of moving support 35
Figure 33: The drawing of assembly 36
Figure 34: Different point of view of assembly 37

Chapter 1: Introduction

1.1 Background

As an essential structure in the skeletal system of our body, bones provide structure and support to bear various loadings. Figure 1 shows the hierarchical structure of bone. Bone tissue is composed of collagen, mineral, and water. Collagen is a protein that provides a soft framework, and calcium and phosphate are minerals that add strength and harden the framework. The combination of soft collagen and stiff mineral allows bone to effectively dissipate energy to avoid damages while remaining strong enough to withstand stress.

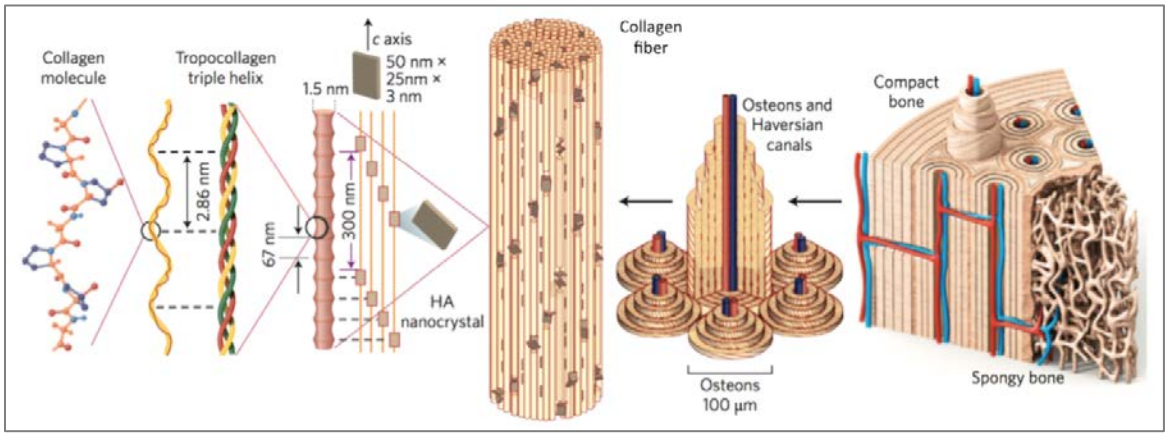

Figure 1: The hierarchical structure of bone [1]

Globally, millions of people of all ages, especially elderly people, suffer from diseases and disorders such as osteoporosis, fracture, or osteomalacia. According to the data from the 2005–2010 National Health and Nutrition Examination Survey (NHANES), 16.2% of adults aged 65 and over had osteoporosis at the lumbar spine or femur neck during 2005 to 2010 [2]. In addition, 48.3% of adults aged 65 and over had low bone mass at the lumbar spine and femur. [2]. The most common bone disease, osteoporosis, is caused by loss of tissue and/or deficiency in calcium or Vitamin D in the human body, as shown in Fig. 2. Losing minerals

causes the bones to become fragile, resulting in weak bones that may fracture easily. Therefore, it is essential to understand bone properties and the process of mineralization.

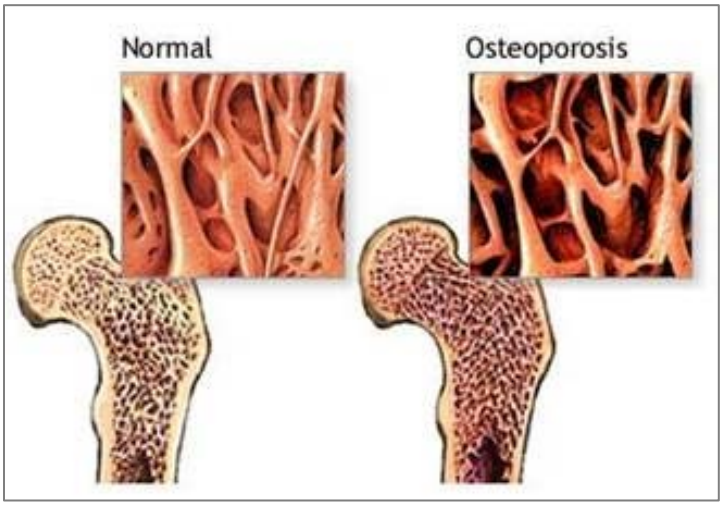

Figure *2*: The comparison of normal bone and osteoporosis bone [3]

Wolff's Law states that the bone of a healthy person or animal will adapt to the loads under which it is placed, as shown in Fig. 3 [4]. The lines in Fig. 3 show that the micro-architecture of trabecula forms along the direction of the loads applied to the bone. However, how the mechanical loading is converted to a physiological signal in a way to arrange the bone itself into the direction of the applied force is still unknown. When the bone remodels, bone forming cells first secret the collagen molecules to build a structural matrix, which is strengthened by the subsequent mineral deposition. By studying the bone mineralization process, in the short term, the process of bone buildup and breakdown can be understood deeply; in the long term, artificial applications can be developed for different types of bone disease.

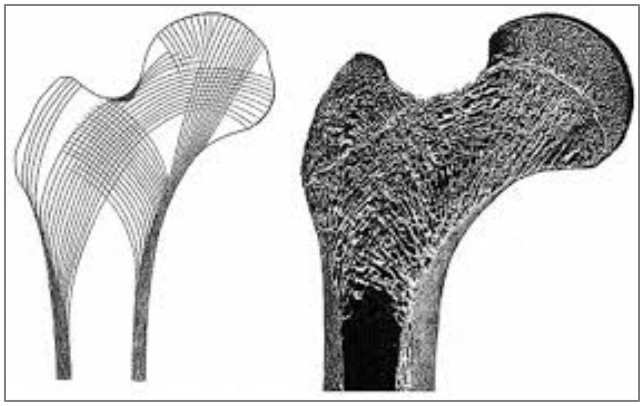

Figure 3: Wolff's Law [4]

1.2 Bone Mineralization

Bone mineralization is composed of two steps: initial mineralization and secondary mineralization, as shown in Fig. 4. The initial stage of mineralization is the bone forming cell mediated process, which is fast to increase the percentage of mineralization rapidly up to 70 percentage of final mineralization within one week [4]. The process of secondary mineralization is much slower, usually requiring more than 6 months to fully develop [4]. The second mineralization needs driving potential to promote a tive transportation of more mineral sources into the existing high mineral concentration of the bone matrix, which is produced as a result of the primary mineralization. However, a lack of knowledge exists to explain the driving force for the transportation against the gradient of mineral concentration.

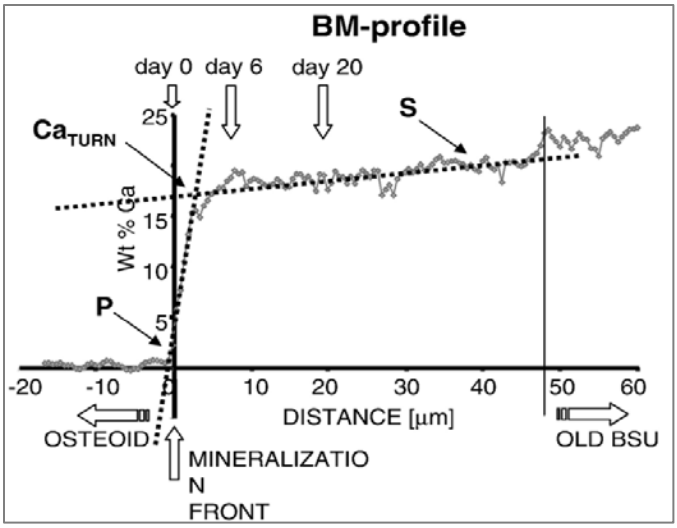

Figure *4*: Diagram of bone mineralization profile of new bone formation [5]

1.3 Hypothesis

It is widely accepted that collagen is involved as a soft framework in the process of bone mineralization. However, the role of collagen is still controversial and the process is not completely understood. Numerous previous studies widely discuss about the bio-chemical interaction of collagen molecules and other compositions, like amorphous calcium phosphate (ACP) and ions. During the formation process of crystalline apatite in the gap zones of collagen fibrils, one widely accepted explanation is that the net charge of collagen molecules in the gap zone provides Coulombic attraction to the penetration of ACP and the arrangement of apatite crystal [6]. Niu's research shows that short-range electrostatic interaction is not the only driving force relevant to the infiltration of ACP. Other types of forces are also responsible for the infiltration of ACP, such as force from skeletal mechanism. Forces from skeletal mechanism act as an external force input in the process of mineralization. Since bone can remodel itself to be stronger to resist to the load bearing, we hypothesize that the mechanoelectric response of collagen to loading can control the kinetic process of intra- and inter-fibrillar mineralization.

Figure 5 shows the hypothetical process of mineralization under an applied external force. Bone is known to possess piezoelectric properties, which is interpreted as the ability of certain materials to generate an electric field in response to an applied mechanical stress. The mechanoelectric response of collagen to external loading may control the kinetic process of intra-and inter–fibrillary mineralization. Bone was treated as a type of material during the experimental, which means bone tested ex-situ has a similar behavior as in-situ

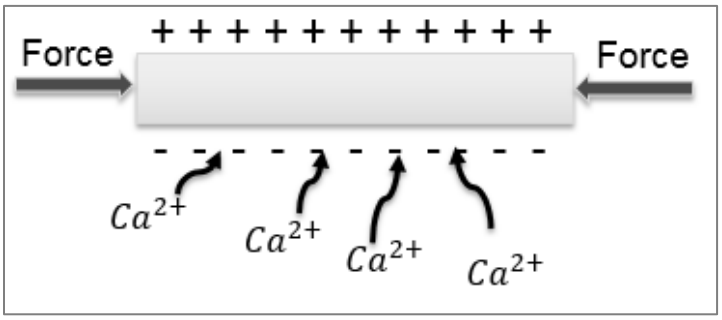

Figure *5*: The general schematic of piezoelectric effect under force

1.4 Objectives

A detailed study of the changes in the morphology and properties of bone in response to external loading stimuli can provide a deeper understanding about the process of bone mineralization. My research has specifically focused on designing a stage with a precise displacement control, integrated into an Atomic Force Microscope (AFM) system. This precise control of displacement requires a piezoelectric motor with a nanometer-scale resolution. A control program has been developed to control the displacement of the stage. Integrated with AFM measurements, the stage designed through this work provides the capability to accurately control an external loading input to various bone tissues. As a final step, bone tissues are characterized while the strain of the sample is varied between 0 and 0.01.

1.5 Description of Atomic Force Microscopy (AFM)

Atomic Force Microscopy (AFM) is a type of scanning probe microscopes that can measure the morphology and local properties of a sample with a nanometer-scale resolution. AFM has three major abilities: imaging, force measurement, and manipulation. High- resolution 3D images can be obtained in air and liquid environments, making AFM largely advantageous over vacuum-based electron microscopes. There are three imaging modes integrated in AFM; namely, contact mode, tapping mode and non-contact mode. Tapping mode was used throughout the entirety of this experiment, as tapping mode minimizes damage to the sample surface and can also prevent sticking of the AFM cantilever tip. The nanometer-scale AFM tip is highly sensitive to forces in the range of pico-Newtons making it a powerful tool for interaction force measurements. These forces between the probe and the samples can be measured as a function of their mutual separation. AFM can also be used as a tool to manipulate distinct nanometer scale structures on a surface.

Figure 6 shows the schematic of AFM. In order to probe a sample surface, AFM uses a micro-cantilever with a very sharp tip at the end to scan over a surface. During the tapping mode operation, the cantilever is harmonically driven at its fundamental resonant frequency by a small piezo element integrated within the cantilever holder while the tip scans over a sample surface. During the process of scanning, the amplitude of oscillations is held contact via a feedback loop. The change in deflection of the cantilever is detected by the laser reflected from the cantilever and recorded on a quadratic photodiode, which is used to construct a 3-D map of the surface morphology. Figure 7 shows the height, amplitude and phase images of a mouse femur obtained in the tapping mode operation. The amplitude image provides a measure of the change in amplitude as tip scans over the surface. The amplitude signal is used to track the surface

topography as shown in Fig. 7a. For the height imaging, the AFM adjusts the distant of the cantilever vertically from the surface to keep the amplitude of the cantilever oscillation as a constant value when scanning over the surface. Fig. 7b shows the height change during scanning. The phase signal is sensitive to surface stiffness and adhesion force between the tip and surface. When the probe encounters regions of different composition, the phase signal changes as shown in Fig. 7c.

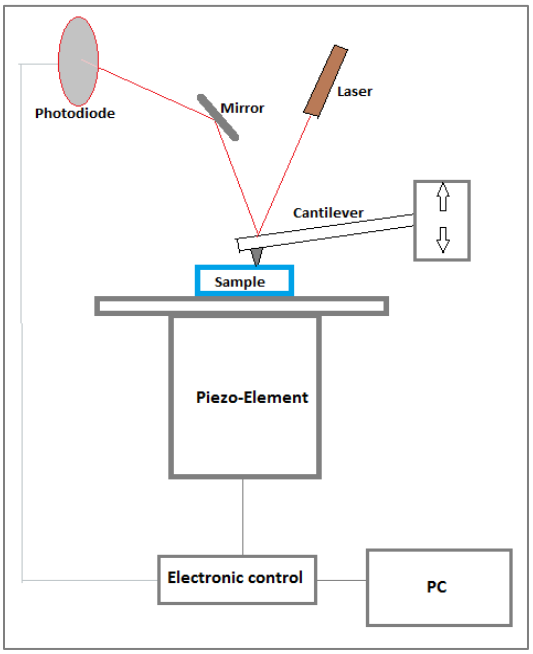

Figure *6*: The schematic of Atomic Force Microscope

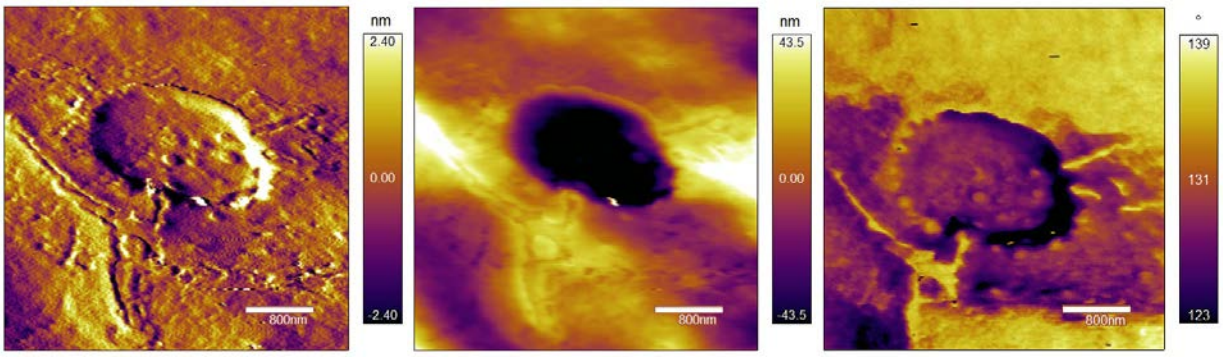

a. Amplitude Imaging b. Height Imaging c. Phase Imaging

Figure *7*: AFM images of the surface of a mouse femur

Chapter 2: Design and Fabrication of Stage

2.1 Constrains

The stage design with a precise displacement control needs to be placed in the limited room under the AFM head as shown in Fig.8. The force the actuator needs to provide ranges from 0-20 N based on Equations 2.1 and 2.2. The actuator with at least micrometer resolution is required to apply a constant force for a desired period of time. In order to eliminate any unbalanced moments acting on the stage, the center of mass of the entire design should be close to the center of symmetry of the AFM stage. Overall, the entire design should be easy to install and the sample holders should be replaceable and removable.

$$F = A * \sigma \tag{2.1}$$

$$\sigma = E * \varepsilon \tag{2.2}$$

Where

$F = force\ applied\ on\ sample$

$\sigma = Strain\ of\ the\ sample$

$E = Young's\ Modulus. MPa$

$\varepsilon = Stress\ applied\ into\ sample$

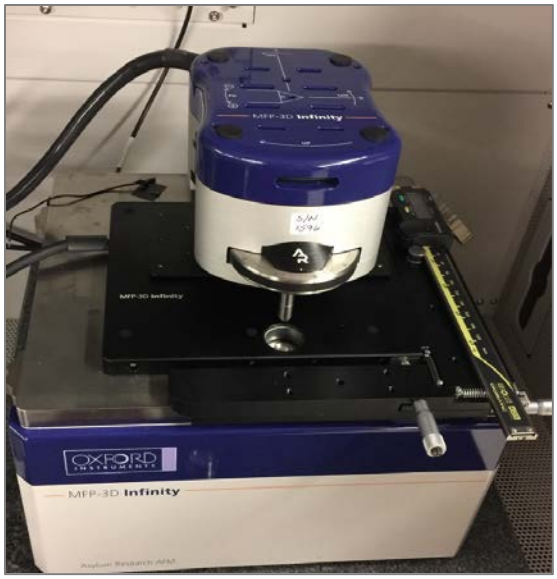

Figure 8: AFM head

2.3.1 Conceptual design

The overall design of the stage consists of three main components; the piezo actuator, controller, and linear translation stage. Figure 9 shows the schematic of the design. The most important constrain is the height under the AFM head. In order to fit the entire design into the AFM system, extensions were used to raise the AFM head, providing a clearance of 26.2mm between the cantilever holder and piezo-scanner as shown in Fig. 10. According to the limitations, the right size of linear translation stage and actuator were purchased. The height of linear translation stage is 22.1mm, which leaves about 4 mm room for support part.

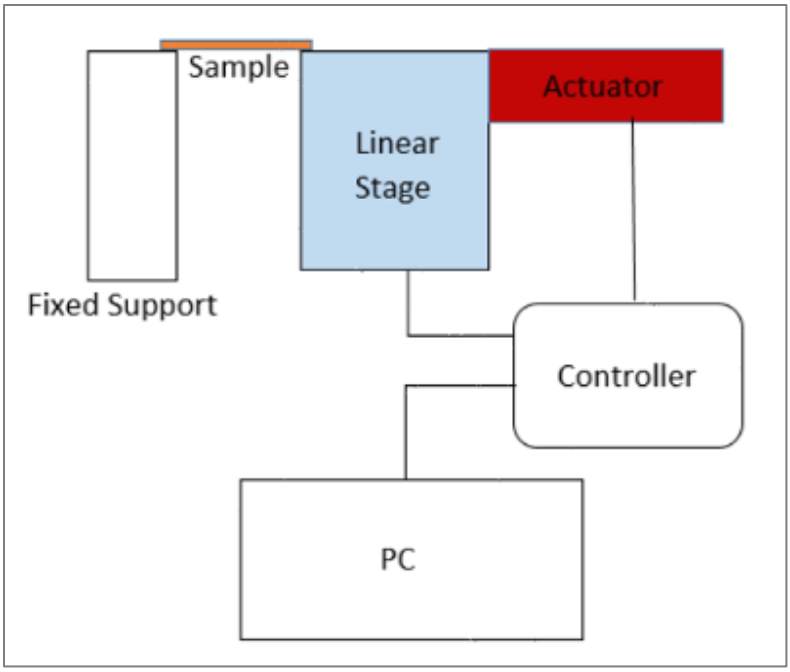

Figure 9: The schematic of the improved design

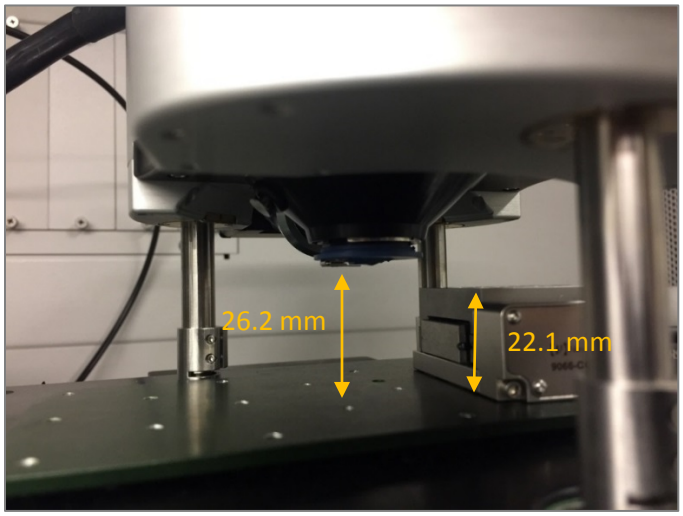

Figure 80: The image of limitation height of AFM head

2.3.2: 3-D Model

Based on conceptual design and the limitations, the 3-D model shown in Fig.11 was built in SOILDWORKS. For convenience, commercially available pin stub specimen mounts was chosen as a sample holder for this design. A set screw with flat head on each side was used to

tighten the sample holders in place to make sure the top surface is always flat. Because of the limited height under AFM head, the moving support part was extended to make sure the end of the pin mount can be fitted into the stage as a raising trigger, shown in Fig.12. All screws used are flat head screw that can locate the position easily and precisely.

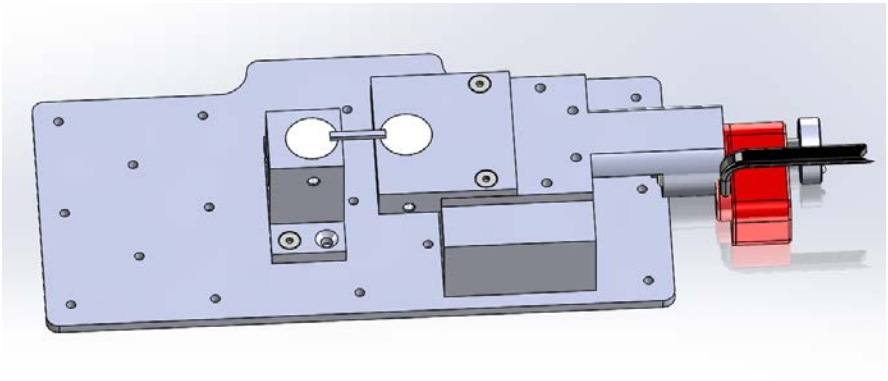

Figure *9*: The isometric view of assembled stage in SOILDWORKS

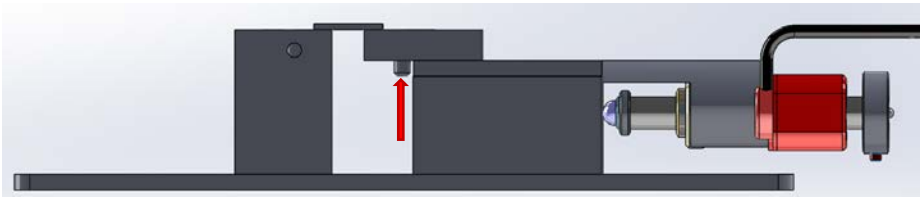

Figure *10*2: The side view of assembly

2.3.3: manufacturing and assembling

After verifying the dimensions of the Solid Works model, parts were manufactured in the machine shop at OSU.

Steps of assembling:

1. The linear translation stage was connected to the plate
2. The actuator was attached to the linear translation stage
3. The moving support was connected to the top of linear translation stage

4. The fixed support was fixed to the plate

The assembled stage was set up as a system with feedback loop shown in Fig.13.

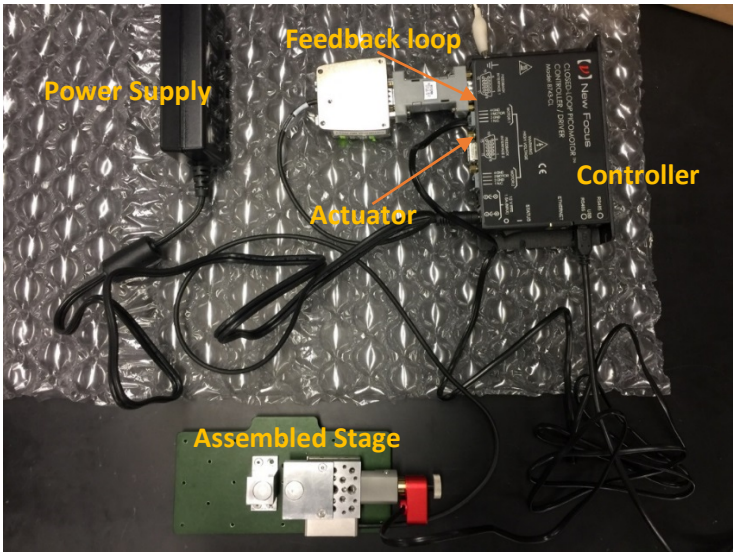

Figure *11*: The connected stage system

2.4 Control program

The schematic diagram of the feedback system is shown in Fig.14. The red color flow chart stands for actuator and the blue color flow chart represents linear translation stage.

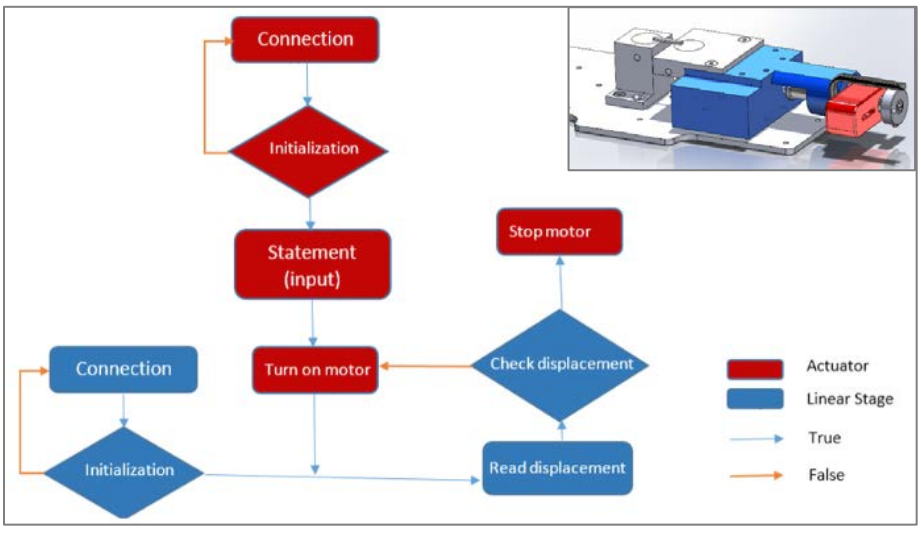

Figure 14: The flow chart of feedback system

2.4.2 The user interface of the program

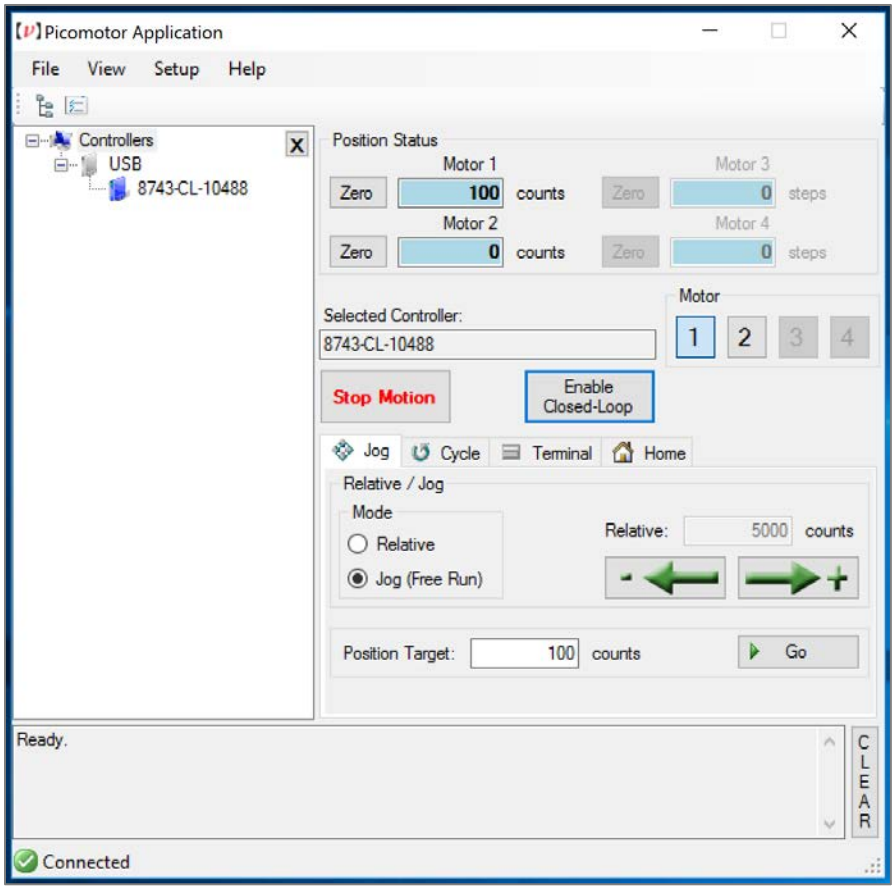

Figure *12*: The user's interface of the program

The default speed of Motor 1 is 2000 steps/ sec, which is equivalent to 40 $\mu m/sec$ in this experiment. Once the system is connected to the computer program, the position of stage is initialized by clicking Zero in Position Status. Counts stands for the number of steps the actuator moves. The desired distance is entered in Position target. Enable Closed-Loop should be enabled before clicking Go. The real position will be shown in Position Status. If the real value is not the desired value, however, the actuator will adjust itself to achieve the desire position.

Chapter 3: Introduction of equipment

3.1 Atomic Force Microscopy (AFM)

Tapping mode is chosen to probe the morphology of samples in this experiment. The design stage is integrated into AFM system by placing it under the AFM head.

3.2 Actuator

The resolution of the 8321 Picomotor actuator from Newport is higher than 30 nm with 12.7 mm travel range, and can exert up to 22 N. Figure16 shows the relationship between the loading force and average step size which is interpreted as the resolution of the piezo-actuator. As the loading force increases, the average step size decreases. In this experiment, the force applied is about 1 pound-force. The resolution can be considered as a constant value of 20 nm during this experiment based on Fig.16,

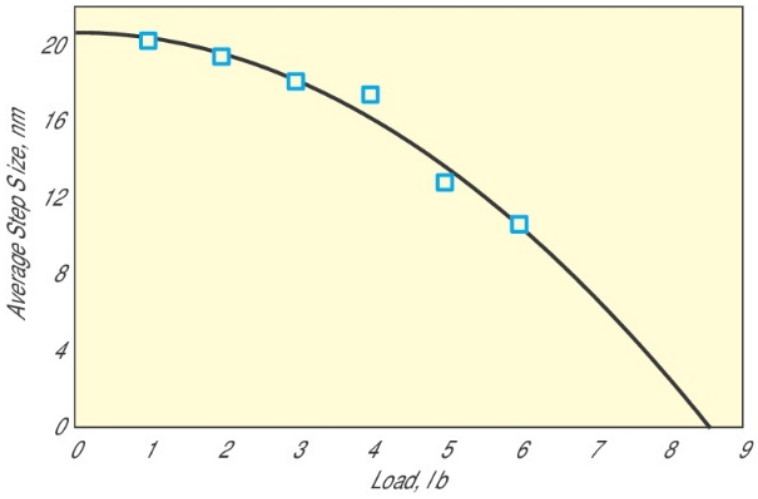

Figure *13*: The resolution of actuator corresponding to different load [7]

3.3 Linear Translation Stage and controller

The first function of the linear translation stage is to provide a linear track, so that the sample can be stretched along its axis. The second function of the linear translation stage is to record the deflection of sample and provide feedback information to the controller. The accuracy of this linear translation stage is within ±80 nm. The Picomotor actuator and the linear translation stage are connected to the controller to create a feedback loop system. Base on the resolution of both linear translation stage and actuator, the overall resolution is 80 nm.

Chapter 4: Characterization

4.1 Test the stage by probing toothpick sticks

Before the bone sample was tested on the design stage, the stage was tested by probing a surface of a toothpick stick made of birch wood. Because the birch wood provides similar mechanical properties as those of bone, it is a good candidate for preliminary scanning. To prepare the sample for AFM characterization, a toothpick stick was flattened by a sand paper to create a flat surface. Different grit sizes of sand papers were applied to create a finer surface. Firstly, a coarse (P320) sand paper was used to move material fast, then a finer (P800) sand paper was used to provide a smoother surface. Finally, P1500 and P2500 sand papers were used to polish the surface. The final length of toothpick stick was 30 mm. The second step was to glue the prepared wood sample to the pin mount, which is integrated with the stage. The sample was dried overnight at room temperature. Figures17 (a) and (b) show the experimental setup for probing the surface of the tooth pick while the sample is mounted on the designed stage. Fig.17 (b) shows the stage firmly attached to the AFM system by the magnetic force generated by the plate.

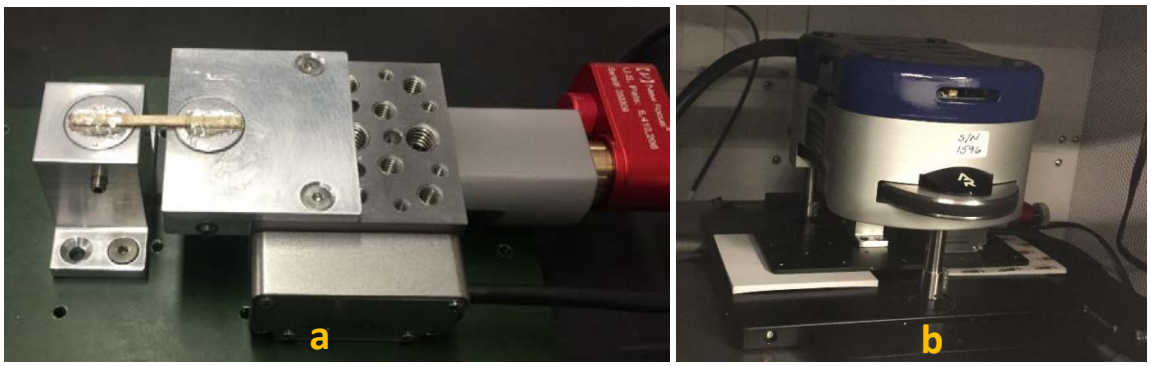

Figure *14*: The experimental setup

The third step was to prepare the setting in AFM to place the cantilever with a sharp tip over the sample and engage it to the surface. The optical microscope image of the AFM

cantilever placed over the prepared sample is shown in Fig.18. The blue light on the cantilever indicates the AFM laser that is used to detect the cantilever deflection during scanning.

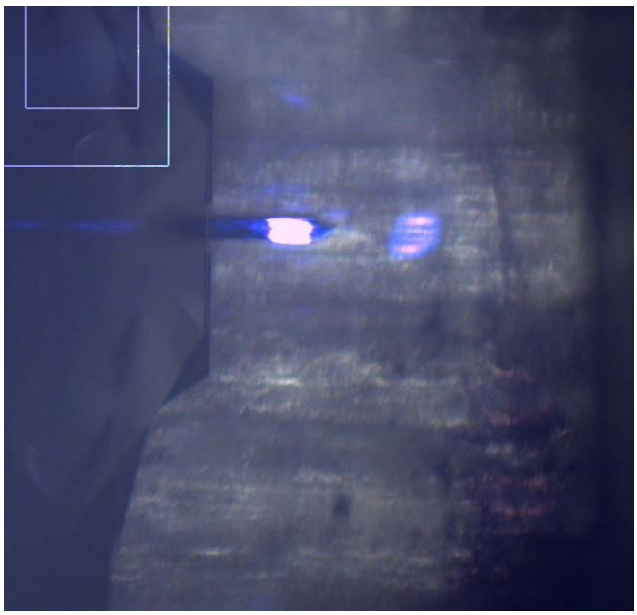

Figure *15*: The camera view from AFM

Finally, the AFM tip scans over the sample while the cantilever is excited at its fundamental resonant frequency. To characterize the surface of the wood sample, initially, a topographic map of a $20\ \mu m\ X\ 20\ \mu m$ area was generated without applying any force input to the sample as shown in Fig. 19 (a). Figure 19 (b) shows the topography of the same exact area after applying a 100 count input displacement ($2\mu m$). A comparison of the two results didn't reveal any significant changes qualitatively in the surface morphology or structure. However, from the standpoint of the overall performance of design stage, the AFM was operated without any interference with the stage, ready to test the bone samples.

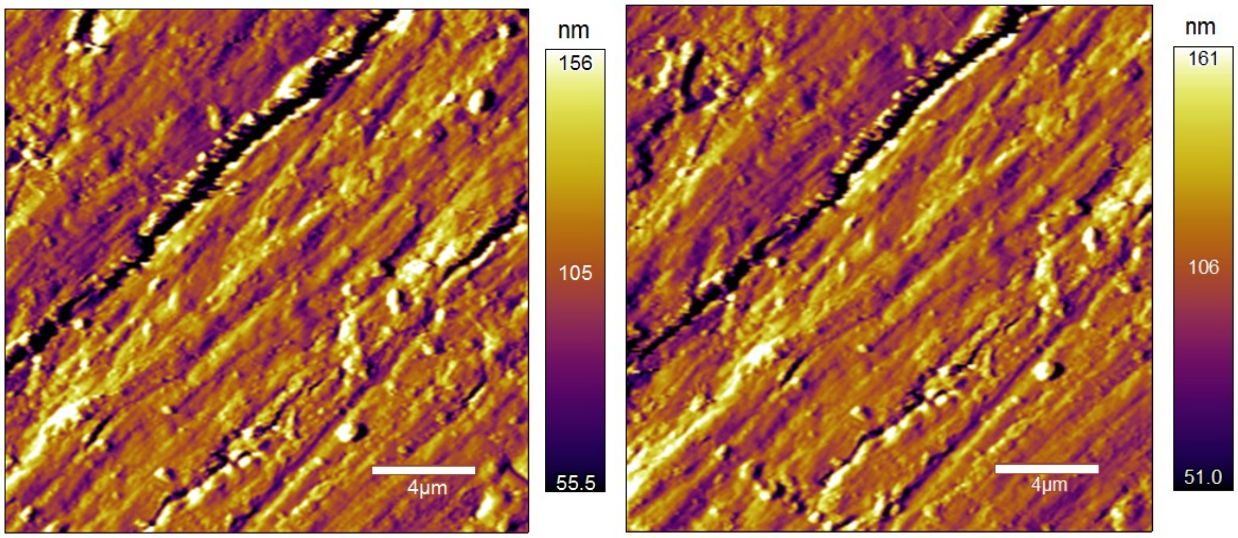

a: Without displacement input b: With displacement input

Figure 19: The morphology of a toothpick without/with displacement input

4.2 Bone sample

A sample from a mouse femur was studied in this experiment. The mouse femur samples were kept refrigerated in saline to prevent bone rotting before the experiment. The average length of the mouse femur is round 14 mm, as shown in Fig.20. Before the experiment, the soft tissue around the bone was peeled off using a tweezer. There are two parts of experiments involving characterization of raw bone and characterization of polished bone. In both parts, the same cantilever and settings were used throughout experiments.

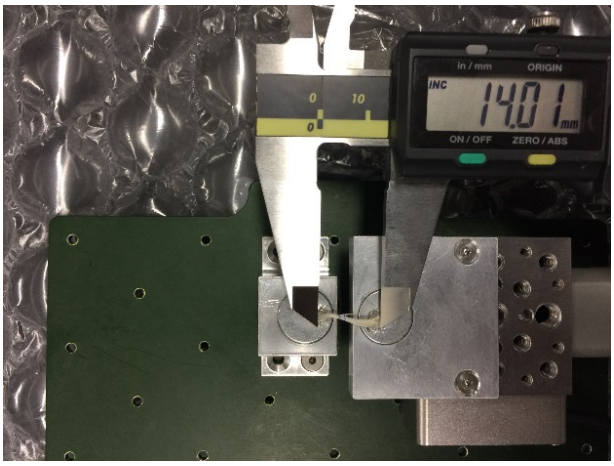

Figure *16*: The dimension of mouse femur

4.2.1 Raw bone sample

In this experiment, the first step was to glue the raw bone to a pin mount when the soft tissue is peeled off using a tweezer. The glued raw bone was placed in air for four hours to dry. Figure 21b, shows the morphology of the mouse femur directly, for a $10\ \mu m\ X\ 10\ \mu m$ scan area. Figure 21a provides more details of Overall morphology change of mouse femur. The surface looks very flat with some special traits. The cell-like trait located at the middle bottom of the frame was chosen for further characterization in Fig. 22.

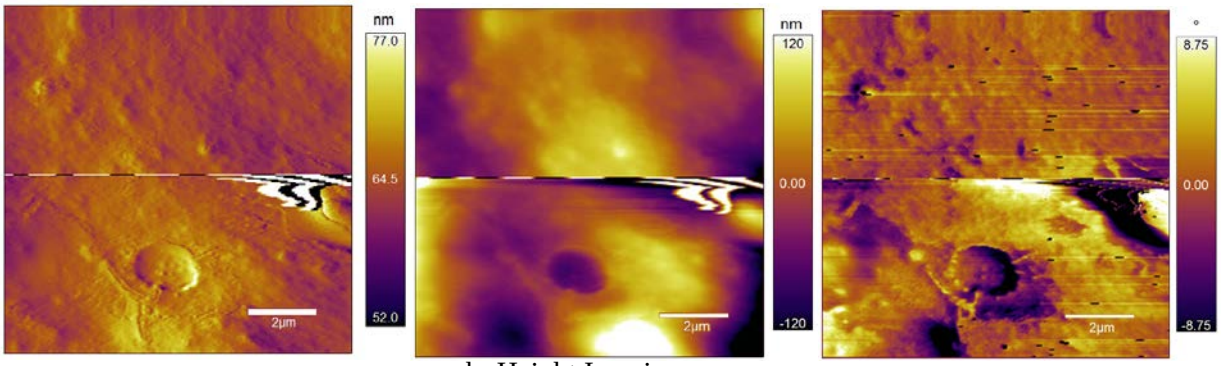

a: Amplitude Imaging b: Height Imaging c: Phase Imaging

Figure *17*: the morphology of mouse femur without 1 μm input

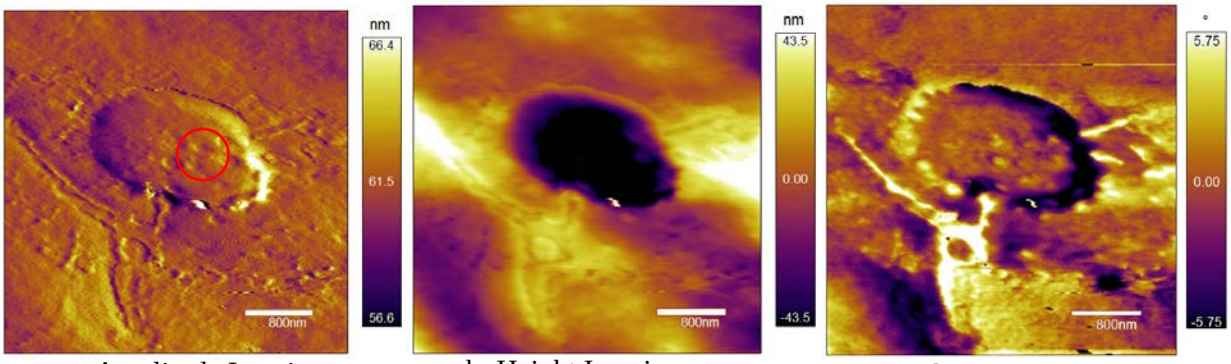

a: Amplitude Imaging b: Height Imaging c: Phase Imaging

Figure *18*: The morphology of mouse femur without 1 μm input (detail)

After finishing scanning of raw bone without a stain input, a 100 count (1 μm) displacement was applied. The location of the cell-like trait changed due to the deflection of bone caused by the strain input. In order to locate the cell-like trait, a larger 15 μm X 15 μm area was scanned in Fig. 23. The location of cell-like trait moved to right since the force is applied on the right side. Compared Fig. 24 with Fig. 22, the cell-like trait is deformed observing the change of circled area in Fig.24.

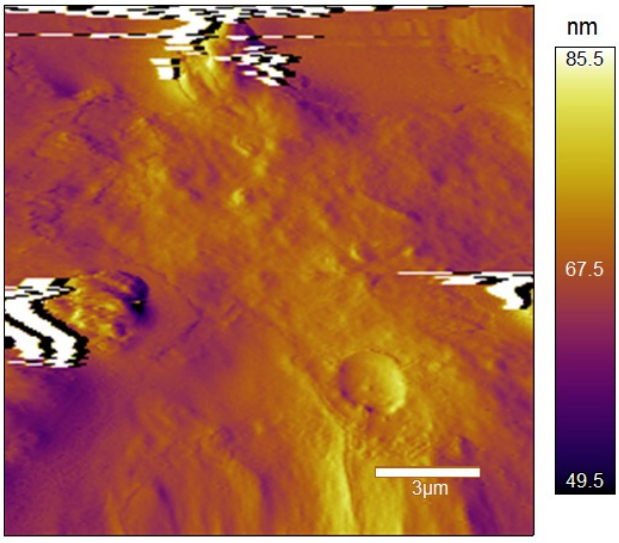

Figure *19*: The morphology of mouse femur with 1 μm input

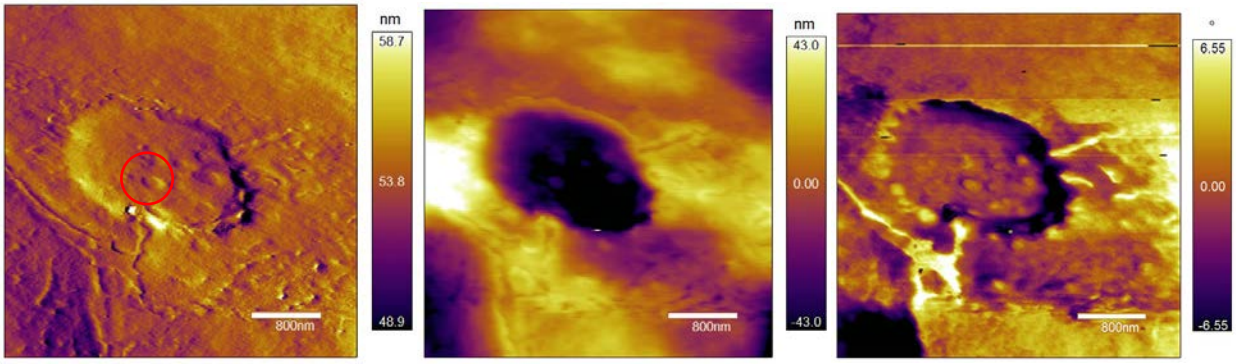

a: Amplitude Imaging b: Height Imaging c: Phase Imaging

Figure *20*: The morphology of mouse femur with 1 μm input (detail)

The artifacts observed in Figs. 21a and 23a, were caused by an unbalanced moment on the AFM stage. These artifacts were eliminated after placing a weight to balance the designed stage.

4.2.2 Bone sample polished

After the soft tissue was peeled off, the raw bone was polished by a sand paper to make the surface more even to probe. Figure 26 (a) shows the polished bone sample and sand paper. The polished bone was then integrated into the stage as shown in Fig.26 (b).

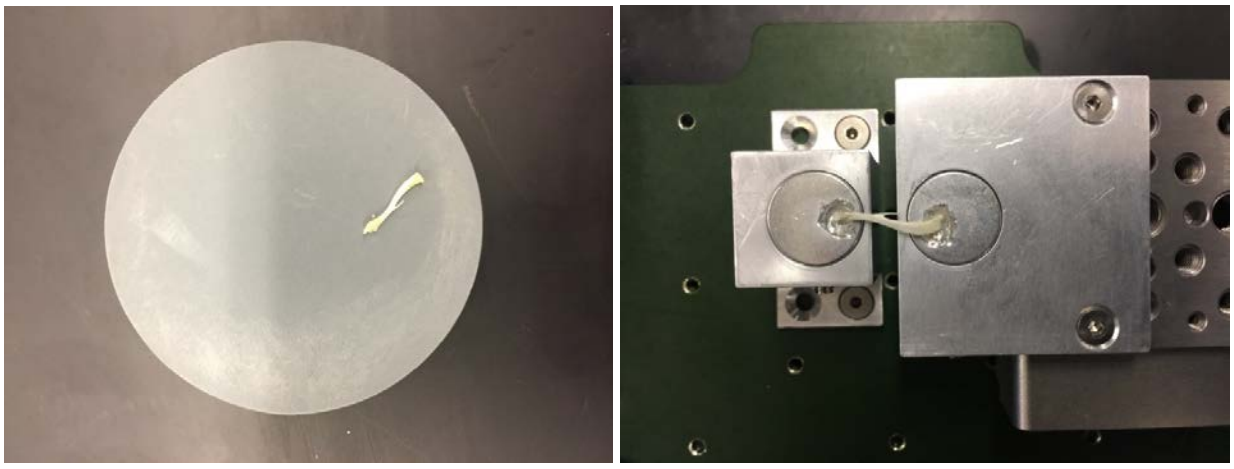

a b

Figure *21*: The setup of stage with mouse femur

Firstly, a 20 μm X 20 μm scan area was probed as shown in Fig.27. In this step, amplitude imaging was used to provide more clear details of morphology change. The cell like trait was chosen for further characterization.

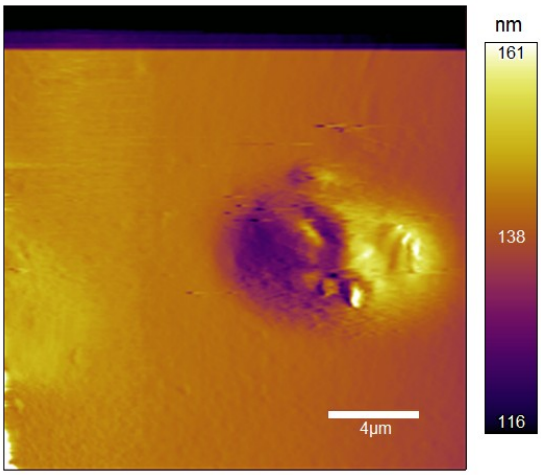

Figure *22*: The morphology of mouse femur without strain input

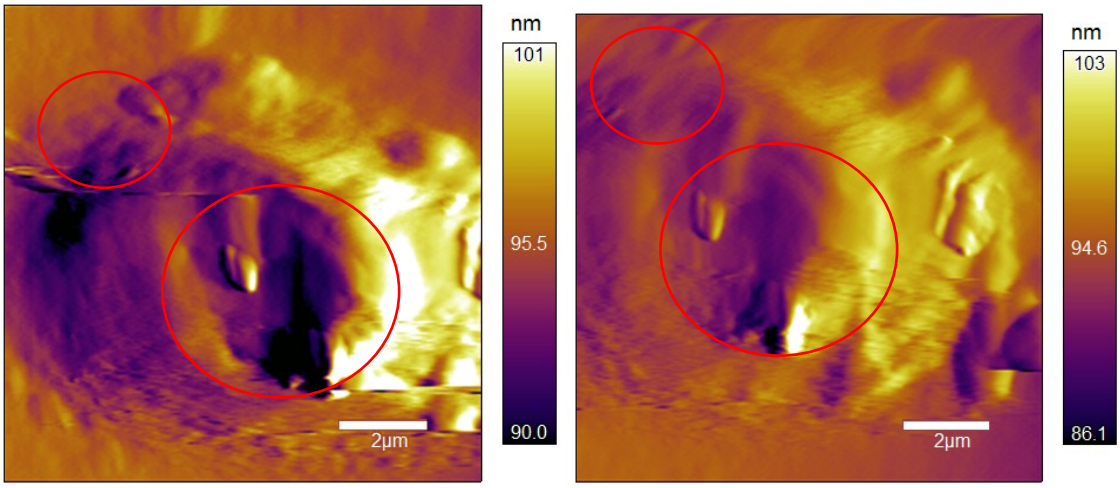

a: Without strain input

b: With strain input

Figure *23*: The comparison of morphology of mouse femur

The morphology with 100 counts (2 μm) in Fig.28 (b) is obviously different with the one in Fig.28 (a) by comparing the circled areas in Fig.28. As evident from the figure, the input strain resulted in the deformation of the feature. Future studies will focus on how the stress affects the bone mineralization.

Chapter 5: Summary

A stage with a precise displacement control had been integrated into an AFM system without interfering with the AFM control. The feedback loop in the control system provides a precise displacement input to the sample. The changes of bone morphology can be characterized with the nanometer scale resolution using AFM when the bone sample is under a strain.

Chapter 6: Future Work

6.1 Improvement of the stage

The design with precise displacement control can be integrated into AFM without any interference with the AFM control. It can also work consistently well, providing strain input. However, in this design shown in Fig.29, removing the sample is done by raising the right pin mount, which sometimes may cause the sample to break. To reduce the possibility of causing failure of sample, a slot will be made in the future design shown as right part in Fig. 30. In order to measure the force applied on sample directly, a loading cell will be integrated into the current stage. In addition, in this design, after strain is applied, it is hard to track the location of the scanning area in small scale. Ideally, the goal is to keep the middle point of the sample static after applying strain.

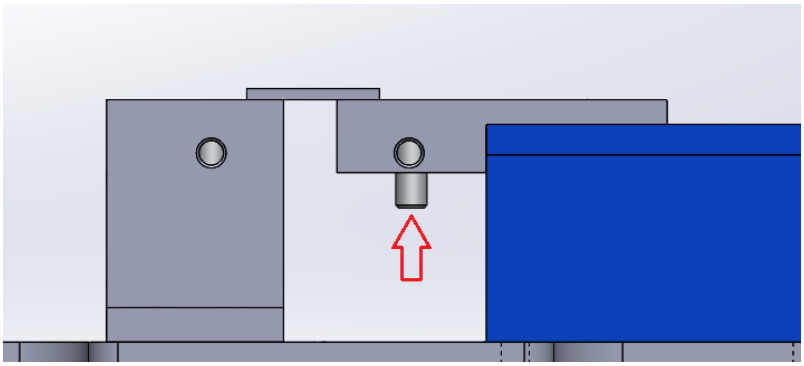

Figure *24*: The front view of the stage

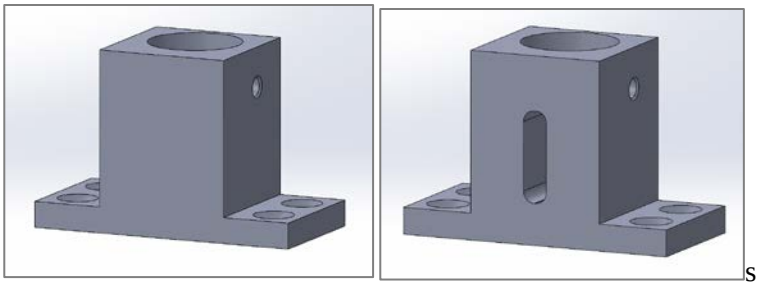 s

Figure *25*: The comparison of designs

6.2 Characterization and analysis of bone

Based on the process of characterization in this research, a more detailed morphology of bone surface at different locations will be imaged with varied applied strain for further analysis. On the other hand, in order to understand the process of bone mineralization with varied applied strain, raw bone should be demineralized first. After that, the morphology of demineralized bone soaked in mineral saline solution will be probed under varied applied strain. In addition, in the future work, the morphology of bone surface will be quantified in MATLAB and the change of morphology will be compared based on quantified data in MATLAB. In addition, force sensor will be integrated into the stage to measure the actual force directly.

Bibliography

[1] Wegst, UltrikeG.K. "Bioinspired Structural Materials." Nature Materials. Nature, 26 Oct. 2014. Web. 15 Mar. 2017

[2] Laura, A and Debra J. "Depression and Obesity in the U.S. Adult Household Population, 2005–2010." NCHS Date Brief, Oct. 2014. Web. 15 Feb. 2017.

[3] Admin. "12 Types Of Bone Diseases And Disorders –A Guide For Patients." Joint Essential. N.p., 18 Oct. 2013. Web. 10 Mar. 2017.

[4] Ruff, Christopher, Brigitte Holt, and Erik Trinkaus. "Who's Afraid of the Big Bad Wolff?: “Wolff's Law” and Bone Functional Adaptation." Wiley Online Library. InterScience, 19 Jan. 2006. Web. 2 Dec. 2016.

[5] P. Roschger, and E. P. Paschalis. "Bone Mineralization Density Distribution in Health and Disease." ELSEVISER, 12 Oct. 2007. Web. 5 Nov. 2016.

[6] Nudelman, Fabio. "In Vitro Models of Collagen Biomineralization." Elsevier. N.p., 15 Apr. 2013. Web. 2 Mar. 2017.

[7] Newport. N.p., n.d. Web. 20 Feb. 2017.

Appendix

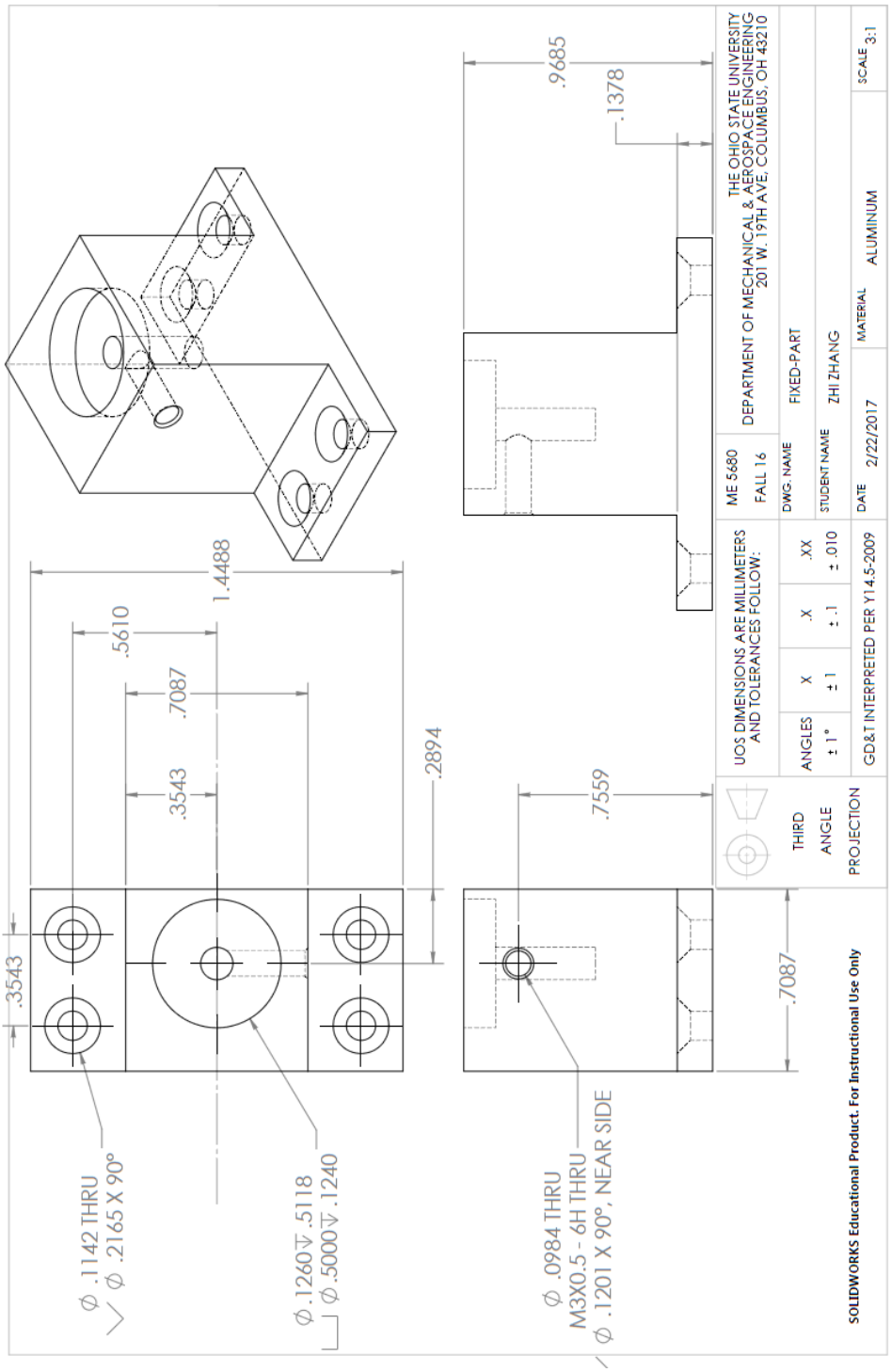

Figure *26*: The drawing fixed support

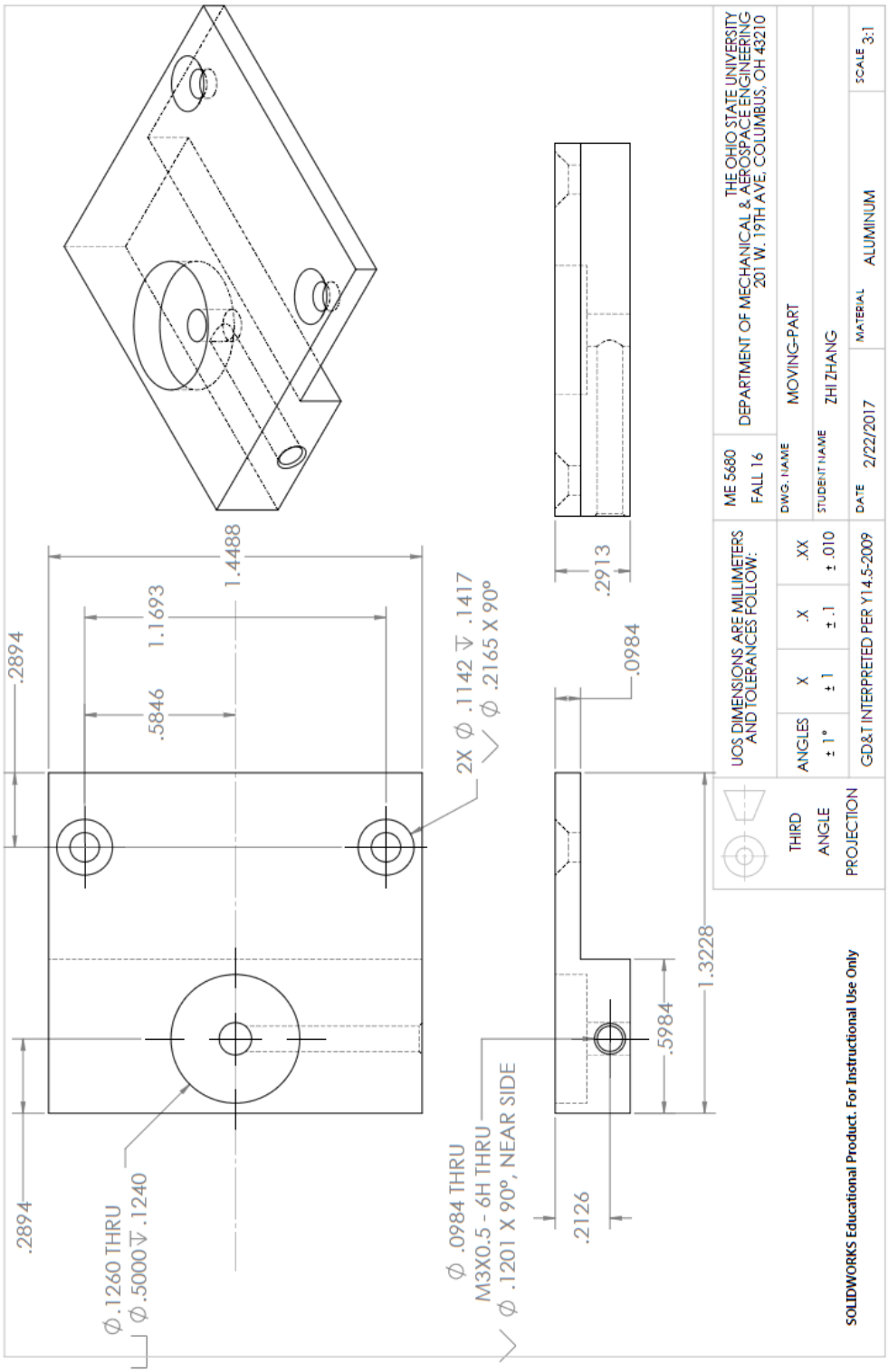

Figure *27*: The drawing of moving support

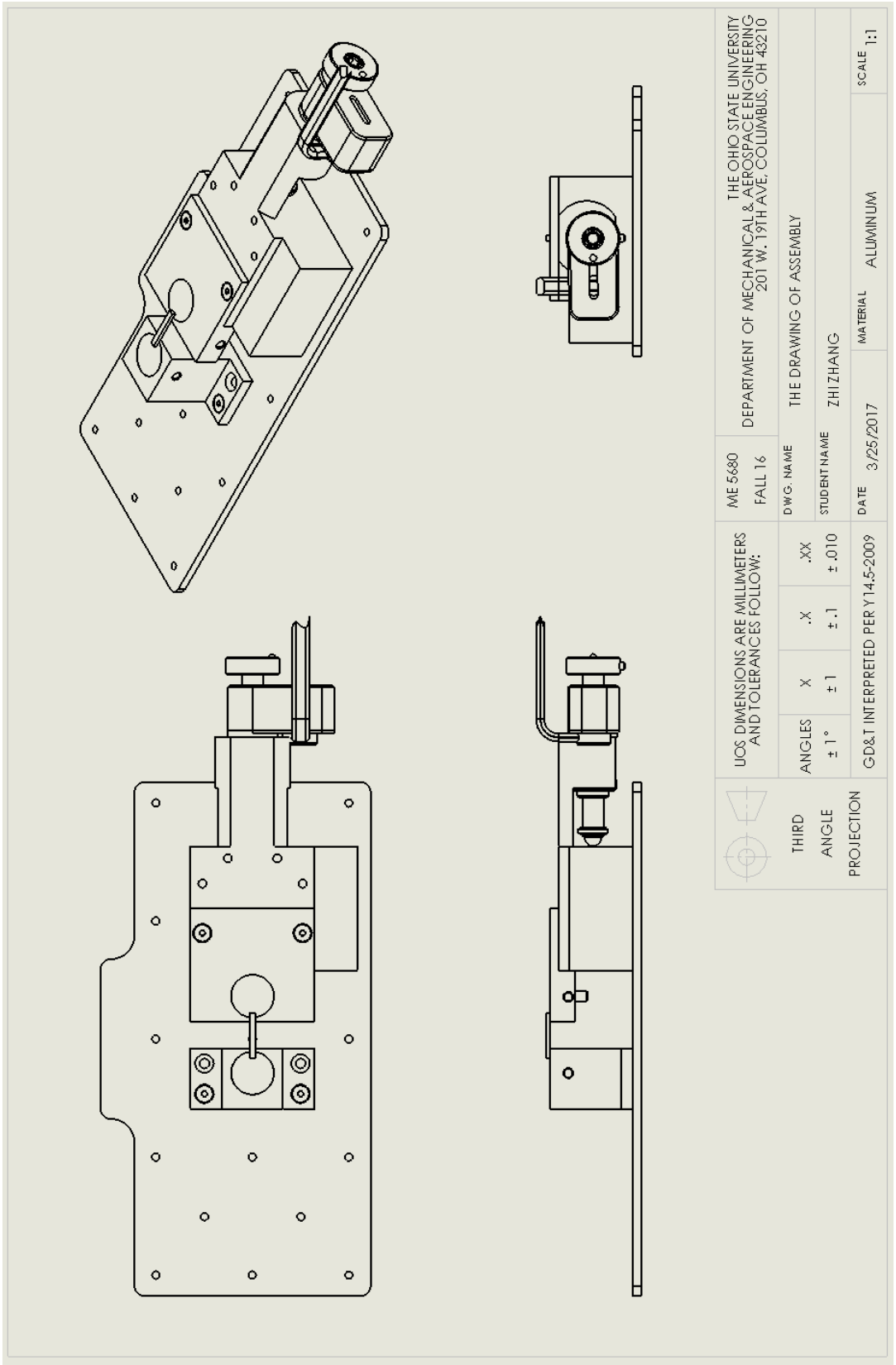

Figure *28*: The drawing of assembly

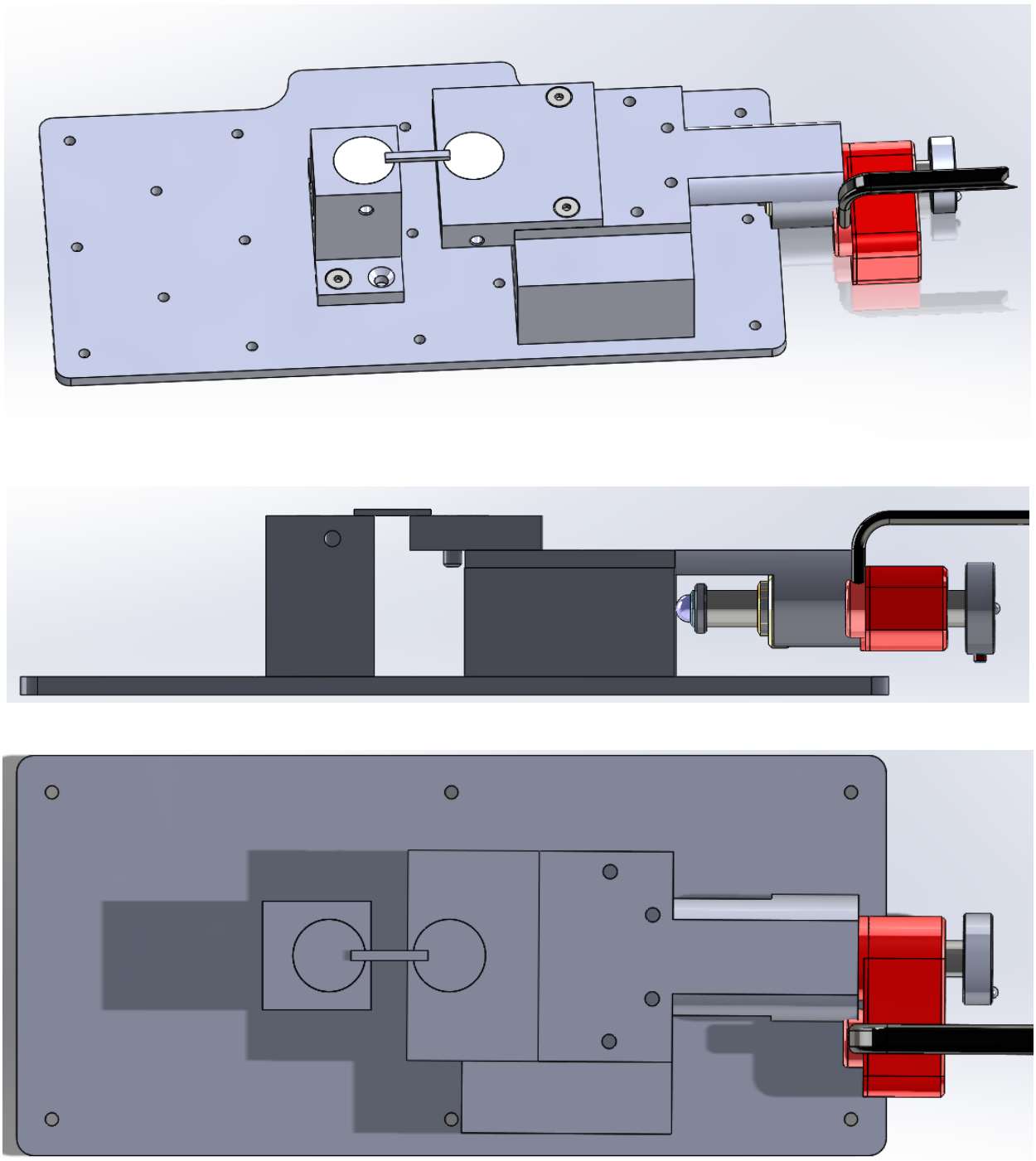

Figure *29*: Different point of view of assembly